VIII International Conference on Particle-Based Methods
PARTICLES 2023
U. Perego, M. Cremonesi, A. Franci (Eds)

IMPROVING ASPHALT DISCRETE NUMERICAL MODELLING WITH REALISTIC PARTICLE SHAPES

R. MICAELO [1a], N. MONTEIRO AZEVEDO [2] AND G. CÂMARA [1b]

[1] CERIS, Dept. Civil Engineering, School of Science and Technology
Universidade NOVA de Lisboa
2829-516 Caparica, Portugal
e-mail: [1a] ruilbm@fct.unl.pt; [1b] g.camara@campus.fct.unl.pt, www.fct.unl.pt

[2] Concrete Dams Dept.
National Laboratory for Civil Engineering
1700-066 Lisbon, Portugal
email: nazevedo@lnec.pt, www.lnec.pt

Abstract. Micromechanical modelling based on the Discrete Element Method (DEM) has been widely used to investigate asphalt behaviour due to its ability to represent an irregular microstructure with variable-sized aggregates, bitumen and voids. The 3D rigid particle models with randomly distributed spherical particles and adopting elastic and/or simple viscoelastic models at the contacts are the standard approach, however, in recent years, a significant research effort is noted to incorporate real particle morphologies in the numerical models.
In this study, a previously developed 3D DEM model of asphalt employing a generalised Kelvin contact model formulation for the viscoelastic contacts is further improved with realistic particle shapes representing the coarse aggregates. A digital library of aggregate shapes was created from the X-ray computed tomography (CT) scan of an asphalt specimen, using an adaptive image-processing method to separate the aggregates in the CT images and the Delaunay triangulation method to define the aggregate 3D surface model. Several virtual aggregates with different sizes were selected from the library to represent the coarse aggregate gradation of the modelled 3D DEM asphalt specimen. Each virtual aggregate is discretized with smaller spherical particles and its deformability is taken into account through the inner particle contacts. The numerical asphalt specimens with realistic particle shapes were submitted to uniaxial tension-compression cyclic tests to determine the stiffness properties, and the results were compared with those of the numerical specimens with all constituents represented by single spherical rigid particles. As shown, the proposed methodology greatly enhances the 3D DEM model's ability to simulate the asphalt behaviour.

Keywords: DEM, Asphalt, Realistic shape, Generalised Kelvin model.

1 INTRODUCTION

Bituminous mixture (asphalt in European terminology) is a composite material made with about 90%$_{v/v}$ aggregates and 10%$_{v/v}$ bitumen that is worldwide used to pave roads and runways. These constituents have to meet defined specifications (e.g. [1,2]). The multi-sized aggregates

coated with bitumen form a packed structure to achieve structural stability and flexibility under different traffic and environmental conditions. However, besides the size distribution of the different aggregate fractions used in the mixture, the shape, angularity and surface texture of particles are controlled because these characteristics affect significantly how individual particles are held within the structure, and therefore the deformation properties of asphalt [3].

The Discrete Element Method (DEM) is a micromechanical numerical approach employed to investigate mechanical properties and damage propagation in asphalt materials. DEM allows for representing the different constituents (aggregates and binder) and modelling their interaction when subjected to time-constant or transient mechanical and thermal effects. The 3D rigid particle models with randomly distributed spherical particles and adopting elastic and/or simple viscoelastic models at the contacts are the standard approach [4], however, in recent years, a significant research effort is noted to incorporate realistic particle morphologies in the numerical models [5]. Several methods have been used to obtain the 3D models of individual particles and to represent them in the DEM assembly. Mollon and Zhao [6] proposed a methodology to generate complex-shaped particles based on the theory of random fields and a Fourier-shape-descriptor, and to build the assembly using a cell-filling algorithm with the Constrained Voronoi Tesselation theory. Differently, Liu et al. [7] scanned individually stone aggregates with an X-ray CT system to build triangulated surface models of particles, and these were filled with small spheres forming a clump. Then, the clumps were generated in the domain and compacted under combined gravity and wall movement to reach a compacted assembly.

In this study, a previously developed 3D DEM model of asphalt employing a generalised Kelvin contact model formulation for the viscoelastic contacts [8] is improved with realistic particle shapes obtained with an image-based method and discretized with small spherical particles. The effect of the enhanced particle assembly characteristics on the viscoelastic stiffness properties measured in uniaxial tension-compression cyclic tests is discussed.

2 REALISTIC PARTICLE SHAPE GENERATION

To incorporate realistically shaped particles in the DEM model, a four-step process was adopted: (i) X-ray CT scanning of the asphalt specimen; (ii) 3D aggregate model extraction; (iii) creation of a digital library of individual aggregate shapes; and (iv) building DEM model of realistically shaped particles.

The X-ray CT scan images of an asphalt specimen obtained in a previous study [9] were herein used. In summary, an asphalt prismatic specimen (40x40x50 mm) was sawn from a cylindrical asphalt specimen (see Figure 1a) and analysed with an XRadia Versa XRM-500 scanner at 160 kV and 63 μA. The pixel resolution of slice images (see Figure 1b) was 45 μm.

To extract the 3D aggregate model from the CT images, the grayscale images were first analysed with the ImageJ software, following a procedure adapted from [10]. Initially, the image brightness was homogenised in each slice image and among the complete image stack to obtain a similar grayscale histogram of the aggregates and bituminous mastic in all of them. Then, a median filter was applied to images without void areas to reduce noise and improve the threshold segmentation quality. The Otsu algorithm was then used to segment the aggregates from the mastic (binder) (see Figure 1c), and a combination of image morphological processing tools was implemented (fill holes, erosion, dilation and watershed) to ease the separation of touching aggregates. To conclude, the complete 3D surface model (STL format) of the

aggregate in the asphalt specimen was built (see Figure 1d).

The STL model was filtered to reduce the initial number of vertices and facets, and then the individual aggregates were exported into individual polygonal models (PLY format) using Meshlab software (see Figure 1e). The exterior surface model of the individual aggregates was redefined with the Delaunay Triangulation method for compatibility with existing DEM tool, and the aggregates were analysed in terms of volume, surface area and dimensions (long, intermediate, and short) using Matlab software. From this collection, several particles graded in defined size fractions (sieve opening 1.0-2.0 mm; 2.0-4.0 mm; 4.0-6.3 mm; 6.3-10.0 mm; 10-12.5; 12.5-16.0 mm) were selected.

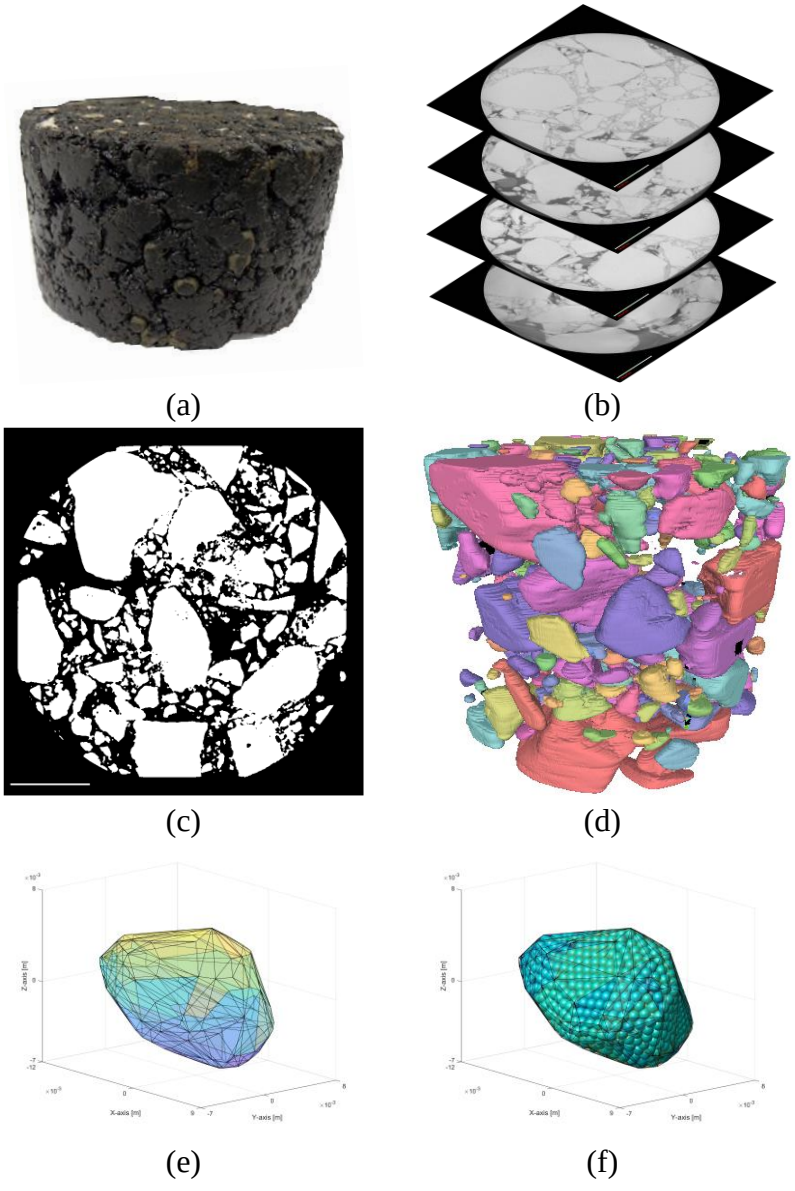

Figure 1: Realistic particle generation: (a) asphalt specimen; (b) CT images; (c) segmented CT image; (d) 3D aggregate structure; (e) individual aggregate model; (f) individual aggregate discretized with inner particles (DEM).

To build the DEM model from the individual aggregate digital models, an algorithm was coded in the DEM program (VirtualPM3DLab). Briefly, each aggregate model is discretized with inner spherical particles with size in a certain range (see Figure 1f). The smaller inner the particles are, the closest the surface of the DEM model is to the original digital model. Also, before the inner particle discretization, the initial aggregate can be scaled to a different size and rotated to a pre-defined or to a random direction.

3 DEM MODELLING OF ASPHALT SPECIMEN

3.1 DEM formulation

The VirtualPM3DLab is a 3D DEM tool programmed in C++ that adopts a conventional spherical particle formulation for solving the law of motion, and the Laguerre-Voronoi diagrams of the spherical particles and the contacts areas to define the contacts to which the force-displacement is applied [11]. Elastic and viscoelastic contact models are implemented in the VirtualPM3DLab program.

In a previous study [8], the 3D DEM tool was used to model the cyclic behaviour of mastic and asphalt specimens and a new explicit 3D generalised Kelvin (GK) contact model formulation was proposed, which allowed to approximate the viscoelastic behaviour of bituminous materials. In this study, the loading simulations of asphalt specimen AM_1 were repeated with different assemblies to evaluate the effect of introducing realistic particle shapes in the 3D DEM model. The simulation conditions and properties were the same as described in [8], namely, the GK model was assumed to be the mastic-mastic and aggregate-mastic contacts and the elastic model to the aggregate-aggregate contacts. The inner contacts of the aggregate particles discretized with multiple smaller rigid spheres were assumed elastic. The inner contacts elastic properties of the aggregate particles were defined in order to reproduce the known aggregate Young modulus (60 GPa).

3.2 Assembly generation

The asphalt specimen modelled is prismatic (50x50x80 mm^3) and the reference assembly of AM_1 [8] (SingleSphere-Ref) is composed of 27646 spherical particles with 160252 contacts. 2739 particles represent the four fractions of the coarse aggregate (2.0-4.75 mm; 4.75-9.5 mm; 9.5-12.5 mm; 12.5-19 mm), and the remaining particles (diameter 1.5-2.0 mm) represent the mastic that is the mixture of fine aggregate and bitumen. The volume proportion is 59.3% aggregate and 40.7% mastic. To generate the assembly, the particles are inserted following the sieve size, from the largest to the smallest.

Two assemblies (RealAgg-1 and RealAgg-2) were generated with the coarse aggregate fraction discretized with smaller spherical particles. 11 aggregate shape templates selected from the digital library, described in section 2, were scaled to use in each aggregate size fraction, inserted randomly in the virtual domain and then discretized with spheres with the diameter of 2.0-4.0 mm (RealAgg-1) and of 1.5-2.0 mm (RealAgg-2). To reduce the time consumed in the generation process, it was defined a maximum number of attempts to insert each aggregate particle and a minimum of 5 spheres to discretize it.

RealAgg-1 contains 38255 particles and RealAgg-2 contains 62950, which corresponds to an increase of 38% and 128% in the number of particles. The average number of spheres per

aggregate particle is 43 and 204 in RealAgg-1 and RealAgg-2, respectively. Figures 2a, 2b and 2c compare the assemblies (SingleSphere-Ref, RealAgg-1 and RealAgg-2) with only the three largest aggregate fractions represented, and Figure 1f shows the complete assembly RealAgg-1. The long dimension lines of aggregates (fractions 1-3) of RealAgg-1 shown in Figure 1e demonstrate that the multi-sphere particles are well distributed in the virtual specimen.

However, the volumetric aggregate proportion in virtual specimens is 49.6% and 51.1% in RealAgg-1 and RealAgg-2, respectively, which is significantly lower than that of SingleSphere-Ref. This occurred because some aggregate models could not be inserted within the defined number of attempts and that volume ended up being discretized as mastic. Hence, it is intended to improve the generation algorithm in the near future. Therefore, to allow a fair comparison of the assemblies with the coarse aggregate fraction represented with single spheres and with multiple spheres (realistic shapes), a second assembly (SingleSphere-2) with single spherical particles was generated with a lower aggregate proportion (51.9%) (see Figure 2d, three largest aggregate fractions).

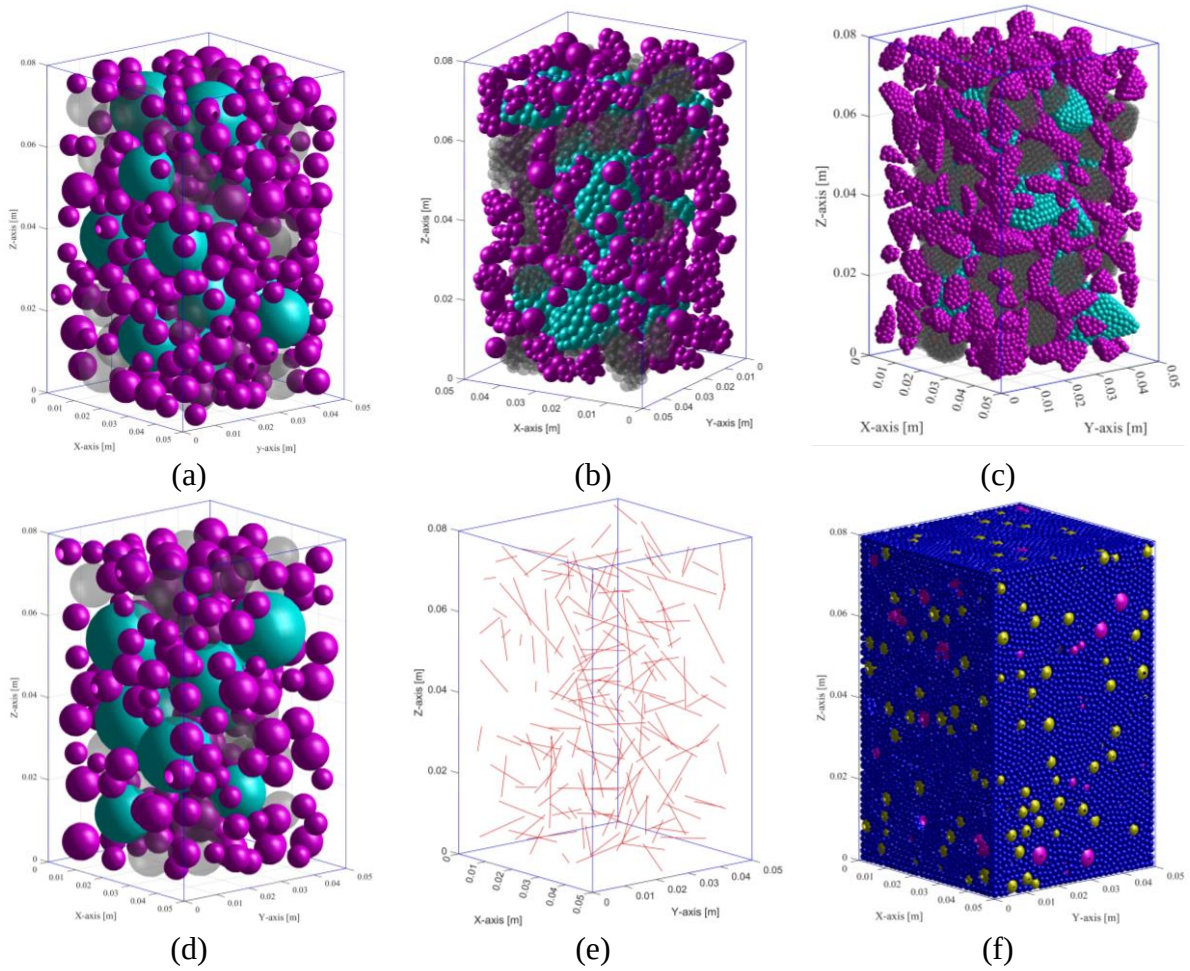

Figure 2: Virtual assemblies: (a) SingleSphere-Ref, aggregate factions 1-3; (b) RealAgg-1, aggregate factions 1-3; (c) RealAgg-2, aggregate factions 1-3; (d) SingleSphere-2, aggregate factions 1-3; (e) RealAgg-1, long dimension line of aggregate factions 1-3 (f) RealAgg-1, complete assembly.

3.3 Viscoelastic stiffness properties

The virtual specimens were subjected to uniaxial tension-compression cyclic loading at various frequencies (2, 5, 10 and 20 Hz) with an imposed strain amplitude of 100 μm/m. The viscoelastic stiffness properties were determined from the applied vertical strain and the normal stress response as:

$$|E^*| = \frac{\sigma_{max} - \sigma_{min}}{\varepsilon_{max} - \varepsilon_{min}} \quad (1)$$

$$\delta = 360 \cdot \frac{\Delta t}{T} \quad (2)$$

where, $|E^*|$ is the norm of the complex stiffness modulus, δ is the phase angle, σ_{max} and σ_{min} are the maximum and minimum stress values in the loading cycle, ε_{max} and ε_{min} are the maximum and minimum strain values in the loading cycle, Δt is the time difference between adjacent stress and strain peaks, and T is the loading period.

Figure 3 shows the variation of the viscoelastic stiffness properties ($|E^*|$ and δ) with the loading frequency for the four virtual specimens. The contact model properties were the same for the four specimens, which were calibrated with the experimental results of the bituminous mixture AM1 in [8]. Overall, the results demonstrate the effect of the coarse aggregate on the asphalt loading response. The specimen SingleSphere-2, with less aggregate content than the reference, had an average decrease of 17% in modulus and an increase of 10% in phase angle. The mastic is a softer material than the aggregate, and the viscous behaviour is more important to the mastic-mastic contacts than to the aggregate-mastic contacts, though both contact types were modelled with the GK model.

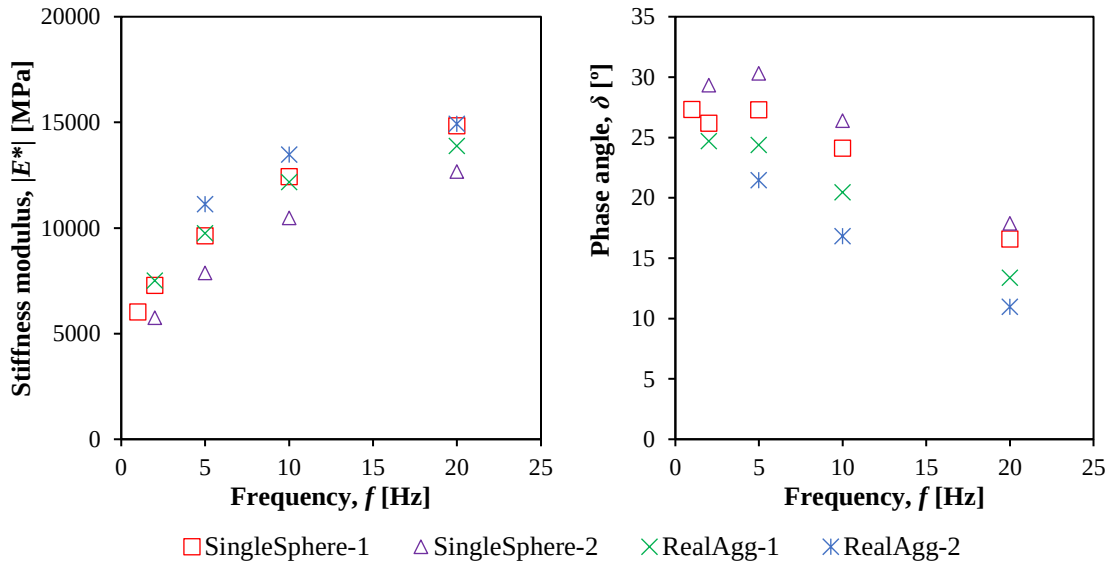

Figure 3: Viscoelastic stiffness properties: (a) $|E^*|$ Vs. f; (b) δ Vs. f

In addition, the incorporation of realistic aggregate shapes and aggregate deformability in virtual specimens increased the stiffness and decreased the phase angle. The stiffness modulus of RealAgg-1 was only on average 2% lower than that of the reference assembly, however, the phase angle decreased by 13% on average. For RealAgg-2, the average variations in the stiffness modulus and phase angle were +8% and -28%. As expected, the irregular aggregate shapes induced a stronger locking structure in the assembly which increased the stiffness and reduced the transversal deformation. This effect was more significant for the assembly with a finer discretisation of the coarse aggregate particles. However, these multiple-sphere particles affected significantly more the phase angle than the stiffness modulus, and the mechanisms contributing to this will have to be further investigated.

4 CONCLUSIONS

The study described in this paper was aimed at improving the ability of a 3D DEM tool to model asphalt materials by incorporating realistic particle shapes in it. A digital library of aggregate shapes was created from the X-ray computed tomography (CT) scan of an asphalt specimen, using an adaptive image processing method to separate the aggregates in the CT images and the Delaunay triangulation method to define the aggregate 3D surface model. In the DEM tool, the aggregates of each size fraction are represented by different shape models from the library, and each virtual aggregate is discretized with smaller spherical particles. The deformability of aggregates is considered through the inner particle contacts. The 3D DEM tool was tested by simulating the loading of a prismatic-shaped asphalt specimen in an uniaxial tension-compression scheme at various loading frequencies. The results demonstrated the importance of introducing irregular aggregate shapes to model the loading and deformation response of asphalt materials. The realistic coarse particle shapes affected more the phase angle than the stiffness modulus, and the mechanisms contributing to this will have to be further investigated.

ACKNOWLEDGMENTS

This work is part of the research activity of the first author carried out at Civil Engineering Research and Innovation for Sustainability (CERIS) and has been funded by Fundação para a Ciência e a Tecnologia (FCT) in the framework of project UIDB/04625/2020.

REFERENCES

[1] IPQ, NP EN 13043:2004/AC:2010. Aggregates for bituminous mixtures and surface treatments for roads, airfields and other trafficked areas, Instituto Português da Qualidade, Caparica, 2010.
[2] IPQ, NP EN 12591:2011 - Bitumen and bituminous binders, Specifications for paving grade bitumens, Instituto Português da Qualidade, Caparica, 2011.
[3] R.N. Hunter, Shelf, Andy, J. Read, The Shell Bitumen Handbook, 6th ed., ICE Publishing, London, 2015.
[4] W. Cai, G.R. McDowell, G.D. Airey, Discrete element visco-elastic modelling of a realistic graded asphalt mixture, Soils and Foundations. 54 (2014) 12–22. https://doi.org/10.1016/j.sandf.2013.12.002.

[5] Y. Li, W. Jiang, J. Xiao, F. Zhao, S. Zhang, C. Xing, D. Yuan, Effects of kneading and impact action on the movement of aggregates in asphalt mixtures during compaction, Construction and Building Materials. 366 (2023) 130210. https://doi.org/10.1016/j.conbuildmat.2022.130210.
[6] G. Mollon, J. Zhao, 3D generation of realistic granular samples based on random fields theory and Fourier shape descriptors, Computer Methods in Applied Mechanics and Engineering. 279 (2014) 46–65. https://doi.org/10.1016/j.cma.2014.06.022.
[7] Y. Liu, X. Zhou, Z. You, S. Yao, F. Gong, H. Wang, Discrete element modeling of realistic particle shapes in stone-based mixtures through MATLAB-based imaging process, Construction and Building Materials. 143 (2017) 169–178. https://doi.org/10.1016/j.conbuildmat.2017.03.037.
[8] G. Câmara, N.M. Azevedo, R. Micaelo, H. Silva, Generalised Kelvin contact models for DEM modelling of asphalt mixtures, International Journal of Pavement Engineering. 24 (2023) 2179625.
[9] R. Micaelo, T. Al-Mansoori, A. Garcia, Study of the mechanical properties and self-healing ability of asphalt mixture containing calcium-alginate capsules, Construction and Building Materials. 123 (2016) 734–744. https://doi.org/10.1016/j.conbuildmat.2016.07.095.
[10] L. Zhang, G. Zheng, K. Zhang, Y. Wang, C. Chen, L. Zhao, J. Xu, X. Liu, L. Wang, Y. Tan, C. Xing, Study on the Extraction of CT Images with Non-Uniform Illumination for the Microstructure of Asphalt Mixture, Materials. 15 (2022) 7364. https://doi.org/10.3390/ma15207364.
[11] N. Monteiro Azevedo, M. Candeias, F. Gouveia, A Rigid Particle Model for Rock Fracture Following the Voronoi Tessellation of the Grain Structure: Formulation and Validation, Rock Mech Rock Eng. 48 (2015) 535–557. https://doi.org/10.1007/s00603-014-0601-1.